DOI: 10.1002/ejic.201100674

Iron(II)-Mediated Reductive Cleavage of Disulfide and Diselenide Bonds: Iron(III) Complexes of Mixed *O,X,O* and *O,X* (X = S, Se) Donor Ligands

Tapan Kanti Paine,[a] Debobrata Sheet,[a] Thomas Weyhermüller,[b] and Phalguni Chaudhuri*[b]

Dedicated to Acharya Prafulla Chandra Ray[‡]

Keywords: Disulfide / Diselenide / Cleavage reactions / Thiophenolate / Selenophenolate / Iron

The syntheses and characterization of a methoxo-bridged di-iron(III) complex, $[Fe_2L^{Se}_2(\mu\text{-}OCH_3)_2(CH_3OH)_2]$ (**1**), and three mononuclear iron(III) complexes $Bu_4N[FeL^{Se}_2]$ (**2**), $Bu_4N[FeL^{Se\prime}L^{Se}]$ (**3**) and $Bu_4N[FeL^{S\prime}L^{S}]$ (**4**) [H_2L^{Se} = 2,2′-selenobis(4,6-di-*tert*-butylphenol), H_2L^{S} = 2,2′-thiobis(4,6-di-*tert*-butylphenol), $H_2L^{Se\prime}$ = 3,5-di-*tert*-butyl-2-hydroxyselenophenol, and $H_2L^{S\prime}$ = 3,5-di-*tert*-butyl-2-hydroxythiophenol] are discussed. The single crystal structure of **1**·7CH_3OH, as determined by XRD, reveals an asymmetric Fe_2O_2 core in which the two iron and two methoxo oxygen atoms constitute a perfect planar atomic arrangement. Complex **1** exhibits a moderate antiferromagnetic exchange coupling (J = –13.2 cm^{-1}) that operates between the two high spin iron(III) centers (S_{Fe} = 2.5) with a resulting S_t = 0 ground state, while **2** is a six coordinate mononuclear high spin iron(III) complex. The mixed ligand complexes **3** and **4** are formed during the reaction of a tridentate *O,X,O* ligand (X = S, Se) with iron(II) salts in the presence of either the $H_2L^{Se–Se}$ or $H_2L^{S–S}$ ligand [$H_2L^{Se–Se}$ = 2,2′-diselenobis(4,6-di-*tert*-butylphenol), and $H_2L^{S–S}$ = 2,2′-dithiobis(4,6-di-*tert*-butylphenol)] in an inert atmosphere, whereby iron(II) is oxidized to iron(III) and the disulfide or diselenide bonds are reductively cleaved. The temperature-independent magnetic moment values of **3** and **4** indicate that the complexes contain mononuclear high spin iron(III) centers. The crystal structure of **3** confirms that a reductive Se–Se bond cleavage with concomitant formation of a five coordinate trigonal bipyramidal anionic iron(III) complex, $[FeL^{Se\prime}L^{Se}]^-$, has occurred. It is proposed that the iron(II) ions take part in the electron-transfer reaction associated with the reductive cleavage of the disulfide and diselenide bonds.

Introduction

The reversible cleavage of disulfide bonds is an important reaction in biological processes such as protein folding, redox reactions and cell signaling.[1] In proteins, the disulfide linkage also acts as a binding site for metals like copper and nickel.[2] The conversion between disulfides and thiolate has been used as a reversible redox process for the development of functional materials. In addition, thio- and seleno-proteins are good catalysts for many redox reactions in biological systems.[1f] Thiols are oxidized to disulfides by oxidizing agents[3] and disulfide bonds are normally cleaved by reducing agents such as borohydrides and alkali metals. Similarly, diselenides can be reductively cleaved with reducing agents like sodium in liquid ammonia, lithium aluminium hydride, and sodium borohydride.[4] Several metal ions can easily oxidize thiols, a process that can then be followed by the complexation of the metal with the resulting disulfide.[5] On the other hand, reductive cleavage of disulfide bonds normally takes place in the presence of low valent metal ions.[6] In spite of the rich coordination chemistry of organodisulfides,[7] reports of the reductive cleavage of disulfide bonds by metal ions are rare.[8]

We have been exploring the transition metal complexes of thio- and selenobisphenol ligands and studying their reactivity.[9] As a natural progression to our earlier work, we have initiated a project to study the coordination chemistry of two new ligands, dithio- and diselenobisphenol (Scheme 1). Herein, we report the syntheses, characterization and crystal structures of iron(III) complexes of a selenobisphenol ligand (H_2L^{Se}) and compared their chemistry with those of iron complexes containing dithio- and diselenobisphenol ligands. We also describe the reductive cleavage of the S–S bond of $H_2L^{S–S}$ during its reaction with an iron(II) salt in the presence of H_2L^{S}. The iron(II) is oxidized to iron(III) during the reaction, which is preformed in an argon atmosphere, with the concomitant formation of a

[a] Department of Inorganic Chemistry, Indian Association for the Cultivation of Science,
2A&2B Raja S. C. Mullick Road, Jadavpur, Kolkata 700032, India
[b] Max-Planck-Institut für Bioanorganische Chemie,
Stiftstrasse 34–36, 45470 Mülheim an der Ruhr, Germany
E-mail: chaudh@mpi-muelheim.mpg.de
[‡] Founder-President of the Indian Chemical Society, on the occasion of the 150th anniversary of his birth

five coordinate mononuclear iron(III) complex, $[FeL^{S'}L^{S}]^-$. The selenium analogue of the disulfide ligand shows Se–Se bond cleavage under similar reaction conditions to yield $[FeL^{Se'}L^{Se}]^-$. The roles of the ligands and of the iron salt in the reductive cleavage of the disulfide and diselenide bonds are discussed.

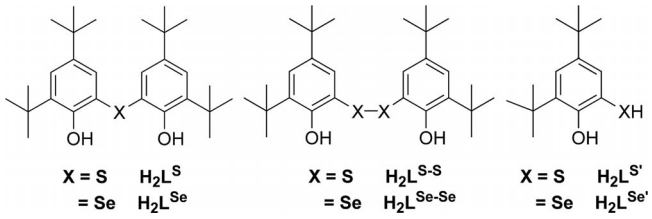

Scheme 1. Ligands used in this study.

Results and Discussion

Ligand $H_2L^{Se–Se}$ was synthesized by reacting 2,4-di-*tert*-butylphenol with selenium and selenium dioxide in a mixture of concd. HCl and concd. H_2SO_4. Ligand $H_2L^{S–S}$ was prepared by reacting 2,4-di-*tert*-butylphenol with S_2Cl_2 in toluene. Both the ligands were characterized by different spectroscopic and analytical techniques (see Exp. Section). The iron(III) complexes were synthesized readily by the reaction of the iron salts with the ligands, as shown in Scheme 2. Reaction, in CH_3OH, of the ligand H_2L^{Se} with $FeCl_2$ produces the bis(μ-methoxo)diiron(III) complex **1**. Addition of excess nBu_4NOCH_3, which acts as a base, to a mixture of CH_2Cl_2, CH_3OH, and **1** yields the homoleptic bisligand mononuclear iron(III) complex **2**. Complex **2** can also be synthesized by reaction, in a nitrogen atmosphere, of the ligand H_2L^{Se} with $FeCl_2$ (2:1) in CH_3CN in the presence of excess nBu_4NOH, followed by exposure of the reaction solution to air.

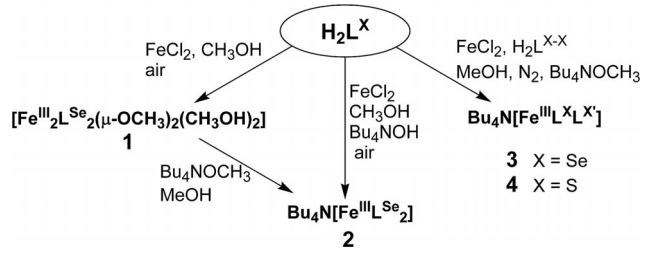

Scheme 2. Syntheses of iron(III) complexes.

Interestingly, ligands H_2L^{Se} and H_2L^S react with $FeCl_2$ in CH_3OH solution under argon and in the presence of their respective diheterobis analogues, $H_2L^{Se–Se}$ and $H_2L^{S–S}$, to yield the mononuclear iron(III) complexes **3** and **4**, respectively. During the reaction, cleavage of the Se–Se and S–S bonds occurs to generate the new ligands $H_2L^{Se'}$ and $H_2L^{S'}$ and thus affording five coordinate mononuclear iron(III) complexes, as shown in Scheme 3. The reductive cleavage of the disulfide and diselenide bonds could not be observed in the absence from the reaction mixture of either the metal ion or H_2L^X ligand.

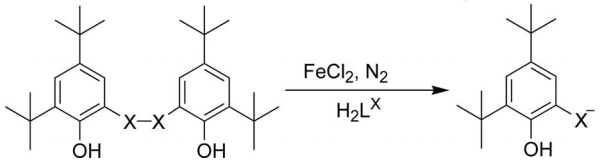

Scheme 3. Reductive cleavage of disulfide and diselenide bonds.

The IR spectra for complexes **1**–**4** confirmed the presence of the ligands in these complexes, as indicated by strong peaks in the 3000–2800 cm^{-1} regions due to ν(C–H) stretches of the *tert*-butyl groups of the ligands, together with other ν(C–H, C=C, C–O) vibrations that were found in the normal wavenumber ranges for these types of linkages.[10] The bands due to the ν(OH) vibrations in the spectra of the free ligands are replaced by broad peaks in the 3200–3400 cm^{-1} regions of the spectra of **1**–**4**, indicating the loss of phenol character of the ligands upon complexation. Two weak but sharp bands at around 1050 cm^{-1}, corresponding to ν(OMe) vibrations, are present in the spectra of **1**, but are absent in the IR spectra of the mononuclear complexes. Except for the μ-methoxo complex **1**, mass spectrometry in the electron impact (EI) and ESI mode was found to be a useful analytical tool for the characterization of the complexes. Mass spectroscopic data recorded in ESI mode for **2**, **3** and **4** do not leave any doubt about the compositions of **2**, **3** and **4**. Two single peaks, one at m/z = 242.2 (in positive mode) and the second at m/z = 1030.5, 827.5 and 732.4 (in negative mode) with the expected isotope distribution pattern calculated for $[Bu_4N]^+$ and $[FeL^{Se}_2]^-$ (**2**), $[FeL^{Se}L^{Se'}]^-$ (**3**) and $[FeL^SL^{S'}]^-$ (**4**) species, respectively.

The optical spectra for complexes **1**–**4** in CH_2Cl_2 have been measured in the range of 300–1000 nm. The bands are of charge-transfer origin, as evident from their high absorption coefficient values.[11] The 450–500 nm regions of the optical spectra for complexes **1**–**4** are dominated by phenolate-to-iron(III) charge-transfer bands.

Single Crystal X-ray Diffraction Studies

Molecular Structure of $[Fe_2L^{Se}_2(\mu\text{-}OCH_3)_2(CH_3OH)_2]\cdot 7CH_3OH$ ($1\cdot 7CH_3OH$)

The crystal structure of $\mathbf{1}\cdot 7CH_3OH$ reveals the presence of the discrete dinuclear molecule shown in Figure 1. Each molecule consists of two iron(III) centers that are related by a crystallographic inversion center. Each iron is coordinated in a facial manner by two *cis*-phenolate oxygen atoms and one selenium atom of the tridentate ligand, and the octahedral environment of each metal center is completed by a pair of methoxy groups that asymmetrically bridge the two iron(III) ions, and one oxygen atom of a coordinated methanol molecule. Two iron and two methoxo oxygen atoms constitute a perfect planar atomic arrangement.

The bridging angles Fe(1)–O(30)–Fe(1)# [106.11(11)°] and Fe(1)–O(30)#–Fe(1)# are equal, as are the O(30)–Fe(1)–O(30)# [73.89(11)°] and O(30)–Fe(1)#–O(30)#

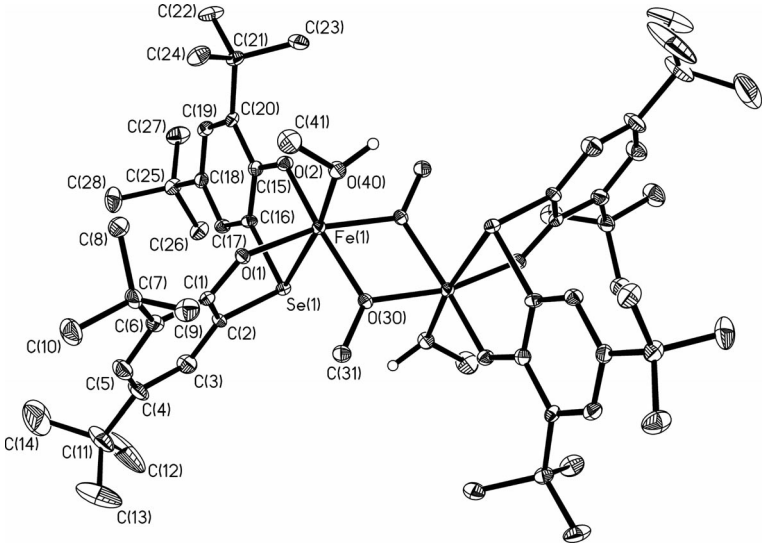

Figure 1. Molecular structure of **1**·7CH_3OH.

angles (Table 1). The dimethoxo bridge is asymmetric, *d*[Fe(1)–O(30)] = *d*[Fe(1)#–O(30)#] = 2.010(2) Å, *d*[Fe(1)–O(30)#] = *d*[Fe(1)#–O(30)] = 1.979(2) Å; Δd = 0.031 Å. A similar asymmetric Fe_2O_2 core has been described earlier by Walker, Poli, and Palaniandavar et al.[12] The bridging Fe–OCH_3, Fe–O(phenolate) [Fe(1)–O(1), 1.940(3) Å; Fe(1)–O(2), 1.927(3) Å] and Fe(1)–O(40) [2.070(3) Å] (where O40 is within a methanol molecule) distances are within the normal range.[13] Both the angles involving the bridging oxygen atoms [106.11(11)°] are equal, as are those involving the iron centers [73.89(11)°], and are typical for an Fe–O–Fe–O ring.[14] The preference of the Fe–O–Fe–O ring for an O–Fe–O angle close to 76° leads to distortions in the remaining angles in the iron coordination sphere altering it from an ideal octahedron. An increase or decrease from the ideal value of 90° occurs for the angles O(40)–Fe(1)–O(30) [98.29(10)°], Se(1)–Fe(1)–O(30) [87.76(7)°], O(40)–Fe(1)–O(30)# [91.65(11)°], and a decrease from 180° is seen for the O(2)–Fe(1)–O(30) [165.37(11)°] and O(1)–Fe(1)–O(30)# [166.87(10)°] angles, making the coordination geometry of the iron a distorted octahedron.

The oxygen of the methanol molecule coordinated to Fe(1), O40, is hydrogen bonded to a noncoordinated methanol molecule. There is a hydrogen bonding network between three other methanol molecules of solvation. The long Fe(1)–O(30) bond is relatively weak because it is *trans* to the stronger, and hence shorter, Fe–O(phenolate) bond, which mitigates the Lewis acidity of the iron center and decreases its affinity for the methoxide bridge. The asymmetry of the Fe–O–Fe–O bridge originates from the *cis*-phenolate coordination of the ligand.

Table 1. Selected bond lengths [Å] and angles [°] for **1**·7CH_3OH.

Fe(1)–O(1)	1.940(3)
Fe(1)–O(2)	1.927(3)
Fe(1)–O(30)	2.010(2)
Fe(1)–O(30)#	1.979(2)
Fe(1)–O(40)	2.070(3)
Fe(1)–Se(1)	2.6476(8)
C(1)–O(1)	1.321(4)
C(15)–O(2)	1.333(4)
Fe(1)···Fe(1)#	3.188(3)
O(2)–Fe(1)–O(1)	96.33(11)
O(2)–Fe(1)–O(30)	165.37(11)
O(1)–Fe(1)–O(30)	93.15(10)
O(2)–Fe(1)–O(30)#	95.99(11)
O(1)–Fe(1)–O(30)#	166.87(10)
O(30)–Fe(1)–O(30)#	73.89(11)
O(2)–Fe(1)–O(40)	92.45(11)
O(1)–Fe(1)–O(40)	92.36(11)
O(30)–Fe(1)–O(40)	98.29(10)
O(30)#–Fe(1)–O(40)	91.65(11)
O(2)–Fe(1)–Se(1)	82.46(8)
O(1)–Fe(1)–Se(1)	82.59(8)
O(30)–Fe(1)–Se(1)	87.76(7)
O(30)#–Fe(1)–Se(1)	94.54(7)
O(40)–Fe(1)–Se(1)	172.35(8)
Fe(1)–O(30)–Fe(1)#	106.11(11)

Molecular Structure of $Bu_4N[FeL^{Se}_2]$ (2)

The crystal lattice of **2** consists of discrete $[Bu_4N]^+$ and $[FeL^{Se}_2]^-$ ions. An ORTEP diagram of the anion with the atom labelling scheme is shown in Figure 2. The central metal ion, iron(III), is in a distorted octahedral FeO_4Se_2 coordination environment. Two tridentate ligands with *O*,*Se*,*O* donor sets bind to the metal in a facial manner. Two phenolate groups and two selenium atoms from two ligands form the equatorial plane in which atoms of the same type occupy *cis* positions. The remaining two phenolate groups are *trans* to each other, and satisfy the hexacoordinate sites. The O(2)–Fe(1)–O(4) and O(1)–Fe(1)–Se(2) bond angles of 156.75(7)° and 171.91(7)°, respectively, are in accord with the distorted nature of the complex, which deviates from an ideal octahedral geometry.

The average Fe–O(phenolate) bond length is 1.912 Å, which is within the range for normal Fe^{III}–O bond lengths. The Fe(1)–O(2) and Fe(1)–O(4) bonds [1.929(2) and 1.934(2) Å, respectively] are a little longer than the upper limit for the range of corrected values (Table 2). This may

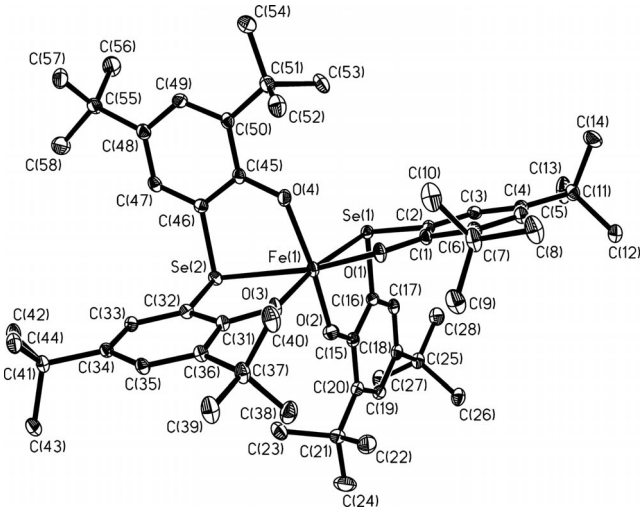

Figure 2. ORTEP representation of **2**.

Table 2. Selected bond lengths [Å] and angles [°] for **2**.

Fe(1)–O(1)	1.892(2)
Fe(1)–O(3)	1.893(2)
Fe(1)–O(2)	1.929(2)
Fe(1)–O(4)	1.934(2)
Fe(1)–Se(1)	2.7966(5)
Fe(1)–Se(2)	2.7797(5)
C(1)–O(1)	1.330(3)
C(15)–O(2)	1.324(3)
C(31)–O(3)	1.324(3)
C(45)–O(4)	1.321(3)
O(1)–Fe(1)–O(3)	102.17(7)
O(1)–Fe(1)–O(2)	100.77(8)
O(3)–Fe(1)–O(2)	93.28(8)
O(1)–Fe(1)–O(4)	93.82(8)
O(3)–Fe(1)–O(4)	101.28(8)
O(2)–Fe(1)–O(4)	156.75(7)
O(1)–Fe(1)–Se(2)	171.91(6)
O(3)–Fe(1)–Se(2)	79.98(5)
O(2)–Fe(1)–Se(2)	86.83(5)
O(4)–Fe(1)–Se(2)	78.09(5)
O(1)–Fe(1)–Se(1)	79.69(5)
O(3)–Fe(1)–Se(1)	170.82(6)
O(2)–Fe(1)–Se(1)	77.54(5)
O(4)–Fe(1)–Se(1)	87.49(5)
Se(2)–Fe(1)–Se(1)	99.43(2)

arise due to the deviation of the complex from the ideal octahedral geometry. The bond lengths and angles in the cation $[Bu_4N]^+$ seem to be reasonable, and are comparable with reported values.[15]

Molecular Structure of $Bu_4N[FeL^{Se'}L^{Se}]$ (3)

Although the analytical and spectroscopic data for **3** unambiguously showed that the mononuclear $Bu_4N[FeL^{Se'}L^{Se}]$ unit is the smallest unit within the structure, a single-crystal X-ray analysis was undertaken to remove any doubts regarding the connectivity within the structure. The structure analysis shows that the lattice consists of discrete $[Bu_4N]^+$ and $[FeL^{Se}L^{Se'}]^-$ ions. The structural analysis confirmed that reductive Se–Se bond cleavage of the $H_2L^{Se–Se}$ ligand occurred during its reaction with the iron(II) salt in the presence of the tridentate facial ligand H_2L^{Se}. An ORTEP diagram of the anion with the atom labelling scheme is shown in Figure 3.

The iron(III) center is in a distorted trigonal bipyramidal $FeSe_2O_3$ coordination environment (τ = 0.77).[16] One ligand with an *O*,*Se*,*O* donor set and another with an *O*,*Se* donor set satisfy the five coordination sites of the iron. Two phenolate oxygen atoms from a H_2L^{Se} ligand and one selenium atom from a $H_2L^{Se'}$ ligand form the equatorial plane, with O(1)–Fe(1)–O(2) and O(2)–Fe(1)–Se(2) angles of 110.57(13) and 125.64(9)°, respectively. The Fe(1)–Se(1) and Fe(1)–O(3) bonds, which are in mutually *trans* positions, form axial linkages with an O(3)–Fe(1)–Se(1) angle of 171.70(9)°. The bond lengths are significantly shorter in **3** than those within the six coordinate complex **2**. The Fe–O bond lengths are consistent with a d^5 high spin electronic

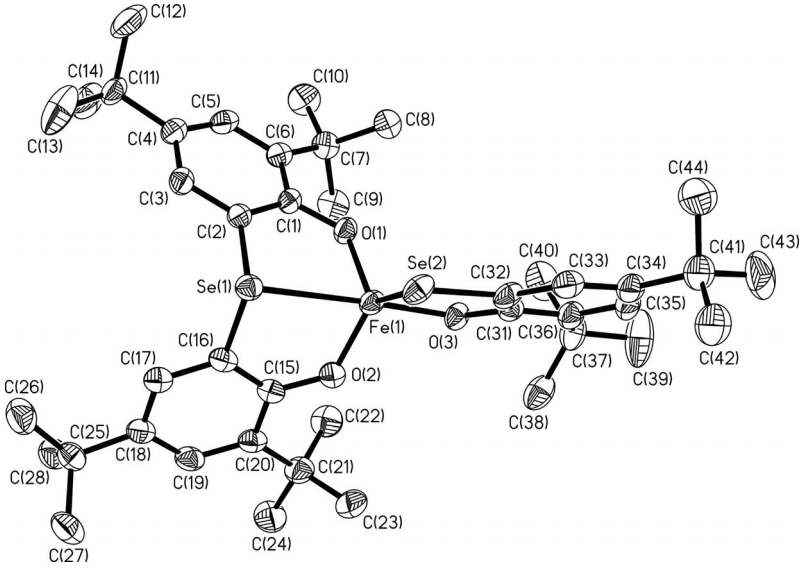

Figure 3. Molecular structure of **3**.

configuration for the iron(III) center (Table 3).[17] The C–C bond lengths of the phenyl rings indicate that the aromatic character of the rings is retained after complexation of the ligands, and that the ligands coordinated to the iron(III) center are dianionic in nature; this leaves an overall negative charge on the iron(III) complex, which is neutralized by a tetrabuylammonium cation.

Table 3. Selected bond lengths [Å] and angles [°] for **3**.

Fe(1)–O(1)	1.886(3)
Fe(1)–O(3)	1.886(3)
Fe(1)–O(2)	1.866(3)
Fe(1)–Se(1)	2.7448(7)
Fe(1)–Se(2)	2.4571(8)
C(1)–O(1)	1.332(5)
C(15)–O(2)	1.345(5)
C(31)–O(3)	1.332(5)
O(2)–Fe(1)–O(1)	110.57(13)
O(2)–Fe(1)–O(3)	100.91(12)
O(1)–Fe(1)–O(3)	104.98(12)
O(2)–Fe(1)–Se(2)	125.64(9)
O(1)–Fe(1)–Se(2)	119.43(9)
O(3)–Fe(1)–Se(2)	86.15(8)
O(2)–Fe(1)–Se(1)	80.86(9)
O(1)–Fe(1)–Se(1)	81.73(8)
O(3)–Fe(1)–Se(1)	171.70(9)
Se(1)–Fe(1)–Se(2)	86.26(2)

Magnetic Susceptibility Measurements

Magnetic measurements for polycrystalline samples of complexes **1**–**4** were done in the temperature range 2–290 K in an applied field of 1 T. The magnetic behavior of **1** is typical for an antiferromagnetically coupled dinuclear complex. At 290 K the μ_{eff} ($\chi_M T$) value is 6.78 μ_B (5.74 $cm^3 K mol^{-1}$), but it decreases with decreasing temperature until it reaches a value of 0.94 μ_B (0.112 $cm^3 K mol^{-1}$) at 2 K, indicating the presence of exchange coupling between the two iron(III) centers (S_{Fe} = 2.5) with a resulting S_t = 0 for the ground state of **1** (Figure 4). Using the Heisenberg spin-Hamiltonian, $\hat{H} = -2J \hat{S}_1 \cdot \hat{S}_2$, for an isotropic exchange coupling between two spins S_1 and S_2, the experimental magnetic data were simulated with a least square fitting procedure[18] with diagonalization of the full exchange coupling matrix, Zeeman splitting and axial zero-field interactions (DS_Z^2) were accounted for if necessary. The solid line in Figure 4 represents the best fit to the data for **1** and was obtained with the parameters: J = –13.2 cm^{-1}, g_{Fe} = 2.0, which are in accord with those for comparable complexes. A comparison of the Fe–O–Fe bridge angles and the Fe–O_{bridge} bond lengths for **1** with those reported in the literature supports the notion that no definitive magneto-structural conclusions based only one of the structural parameters mentioned above can be obtained.[19]

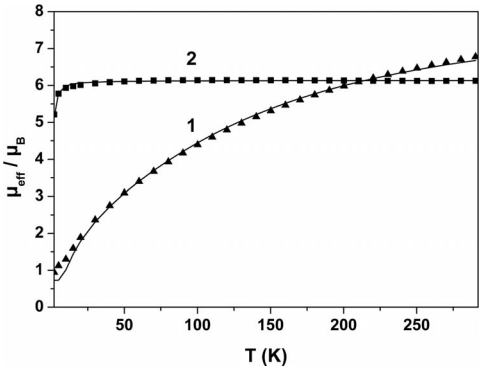

Figure 4. Plots of μ_{eff} vs. T for solids **1** and **2**; the solid lines represent the best fits to the data.

Above 10 K, complexes **2**, **3** and **4** exhibit μ_{eff} values of 6.13 ± 0.04, 5.92 ± 0.06 and 6.01 ± 0.10 μ_B, respectively (see Figures 4 and 5). This clearly shows that the complexes contain d^5 high spin ions, i.e. iron(III). Simulations of the experimental magnetic moment data yield g_{Fe} = 2.074 (θ = –0.39 K) for **2**, g_{Fe} = 2.0 (θ = –0.96 K, TIP = 256×10^{-6} $cm^3 mol^{-1}$) for **3** and g_{Fe} = 2.02 (θ = –0.65 K, TIP = 290×10^{-6} $cm^3 mol^{-1}$) for **4**. A TIP (temperature-independent paramagnetism) value of ca. 300×10^{-6} $cm^3 mol^{-1}$ per ion for high-spin iron(III) has been reported in the literature.[20] The temperature-independent μ_{eff} values indicate the mononuclear nature of **2**–**4**.

Conclusions

The synthesis and characterization of two new bisphenol ligands and their reactivity towards an iron salt are re-

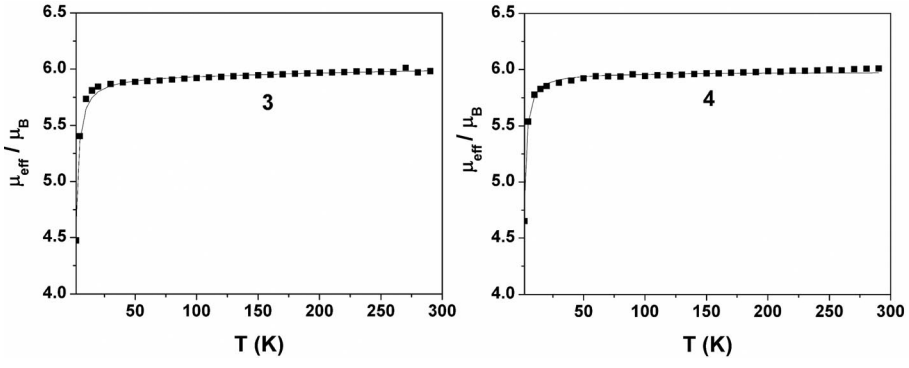

Figure 5. Plots of μ_{eff} vs. T for solids **3** and **4**; the solid lines represent the best fits to the data.

ported. The reductive S–S and Se–Se bond cleavage of dithio- and diselenobisphenols by iron(II) in the presence of tridentate *O*,*X*,*O* donor ligands (X = S, Se) with the concomitant formation of iron(III) complexes, $[FeL^{X}L^{X'}]^{-}$, is discussed. The reactions with the iron(II) salt were performed in an inert atmosphere, but the isolated products are iron(III) complexes, which was established by various spectroscopic analyses. The single crystal structure of the selenium analogue, **1**·7CH_3OH, confirmed that cleavage of the diselenide bond had occurred. It is proposed that the iron(II) takes part in this electron-transfer process, reducing the disulfide and diselenide groups to thiolate and selenolate, respectively. The results described herein have shown the roles of the metal and ligand in the reductive cleavage of disulfide and diselenide bonds. The reactivity of diseleno- and dithiobisphenol ligands with other metal ions is currently being investigated in our laboratory.

Experimental Section

Materials and Physical Measurements: All chemicals were purchased from commercial sources and used without further purification. Solvents were distilled and dried before use. Fourier transform infrared spectroscopy with KBr pellets was performed on a Perkin–Elmer 2000 FTIR instrument. Solution electronic spectra were measured on a Perkin–Elmer Lambda 19 spectrophotometer. Mass spectra were recorded either in the EI or ESI (in CH_2Cl_2) mode with a Finnigan MAT 95 or 8200 spectrometer. Magnetic susceptibilities of the polycrystalline samples were recorded on a SQUID magnetometer (MPMS, Quantum Design) in the temperature range 2–290 K with an applied field of 1 T. The resulting volume magnetization values for the samples had their diamagnetic contributions compensated for and were recalculated as volume susceptibilities. Diamagnetic contributions were estimated for each compound with Pascal's constants. ^{1}H NMR experiments were carried out on a Bruker ARX spectrometer (400 MHz).

X-ray Crystallographic Data Collection and Refinement of the Structures: Dark red single crystals of **1**·7CH_3OH, **2**, **3** were coated with perfluoropolyether, picked up with glass fibers, and mounted on a Siemens SMART diffractometer (**1**·7CH_3OH and **2**) and a Nonius Kappa-CCD diffractometer (**3**) equipped with cryogenic nitrogen cold streams operating at 100(2) K. Graphite monochromated Mo-K_α radiation (λ = 0.71073 Å) was used. Intensity data were corrected for Lorentz and polarization effects. The faces of the crystals of **1**·7CH_3OH and **2** were determined, and the intensity data for these complexes were corrected for absorption with the Gaussian absorption correction method embedded in ShelXPREP,[21a] whereas data for **3** were corrected with SADABS.[21b] The program SHELXL97[21c] was used for the refinement of the structures. All structures were solved and refined by direct methods and difference Fourier techniques. Non-hydrogen atoms were refined anisotropically. Hydrogen atoms were placed at calculated positions in the models and refined as riding atoms with isotropic displacement parameters. Details of the data collections and structure refinements are summarized in Table 4.

Crystals of **3** appeared to be of low quality. The structure refinement revealed that the unit cell contains large volumes filled with extremely disordered solvent, most probably methanol and water molecules, which account for of 22% of the total crystal volume. Attempts to find a reasonable disorder model for the solvent in **3** were not successful. The SQUEEZE[21d] routine in the program PLATON was therefore used to remove diffuse solvent contributions from the data for **3**. The $[NBu_4]^+$ cation and two *tert*-butyl groups of the ligand were also found to be disordered. Two split atoms positions were refined for these moieties, the bond lengths were restrained and equal displacement parameters were applied for the related atoms with the SAME, SADI and EADP instructions of ShelXL97. A total of 172 restraints were used in the refinement of the crystal structure.

Table 4. Crystallographic data for **1**·7CH_3OH, **2** and **3**.

	1·7CH_3OH	**2**	**3**
Empirical formula	$C_{67}H_{122}Fe_2Se_2O_{15}$	$C_{72}H_{116}FeNO_4Se_2$	$C_{58}H_{96}FeNSe_2O_3$
Formula weight	1437.27	1273.48	1069.13
Temperature [K]	100(2)	100(2)	100(2)
λ(Mo-K_α) [Å]	0.71073	0.71073	0.71073
Space group	$P\bar{1}$	$P2_1/n$	$R\bar{3}$
a [Å]	11.3876(8)	16.1348(12)	27.014(2)
b [Å]	13.16808(10)	23.824(3)	27.014(2)
c [Å]	13.7062(12)	19.000(2)	51.115(4)
α [°]	83.28(2)°	90	90
β [°]	86.92(2)°	94.23(2)°	90
γ [°]	88.08(2)°	90	120°
V [Å^3]/*Z*	2037.4(3)/1	7283.6(13)/4	32304(4)/18
Density (calcd.) [Mg m^{-3}]	1.171	1.161	0.989[a]
Absorption coeff. [mm^{-1}]	1.302	1.250	1.257
F(000)	764	2724	10242
θ Range	1.79–27.50°	3.20–30.00°	1.51–23.50°
Reflections collected	17597	24780	28941
Unique reflections	8766 [R_{int} = 0.0423]	17789 [R_{int} = 0.0532]	10449 [R_{int} = 0.0608]
Data/restraints/parameters	8761/0/422	17638/0/749	10449/172/664
Goodness-of-fit on F^2	0.992	1.011	1.019
Final *R* indices [$I > 2\sigma(I)$]	R_1 = 0.0550, wR_2 = 0.1442	R_1 = 0.0449, wR_2 = 0.0953	R_1 = 0.0504, wR_2 = 0.1253
R indices (all data)	R_1 = 0.0848, wR_2 = 0.1570	R_1 = 0.0733, wR_2 = 0.1102	R_1 = 0.0798, wR_2 = 0.1344
Largest diff. peak and hole [e Å^{-3}]	0.93/–0.50	0.50/–0.79	0.38/–0.26

[a] Low density is due to solvent elimination with PLATON/SQUEEZE.[21d]

CCDC-777324 (for **1**·7CH_3OH), -777325 (for **2**) and -777326 (for **3**) contain the supplementary crystallographic data for this paper. These data can be obtained free of charge from The Cambridge Crystallographic Data Centre via www.ccdc.cam.ac.uk/data_request/cif.

Ligand Synthesis: The ligand H_2L^S was synthesized according to a literature procedure.[22] The ligand H_2L^{Se} was synthesized according to a modified version of the method described by Pastor et al.[23]

2,2′-Diselenobis(4,6-di-*tert*-butylphenol), $H_2L^{Se–Se}$: To a suspension of metallic selenium (2.1 g, 27 mmol) and selenium dioxide (1.0 g, 9 mmol) in conc. hydrochloric acid (20 mL), conc. sulfuric acid (2.5 mL) was added drop wise and with constant stirring over a period of 30 min. The reaction was stirred for another 2 h to settle a red oily liquid. Chloroform (15 mL) was added to the mixture. Then a mixture of 2,4-di-*tert*-butylphenol (3.6 g, 17 mmol) in chloroform (15 mL) was added drop wise with a syringe and the reaction mixture was stirred for another 8 h at room temperature. The resulting solution was filtered through a celite bed, the filtrate was washed with brine solution, and the organic part was dried with anhydrous sodium sulfate and concentrated in vacuo. A brown solid emulsion was formed that was subjected to column chromatography with hexane to give a brown solid. The brown solid was recrystallized from a methanol/hexane (1:1) mixture to afford $H_2L^{Se–Se}$ as a yellow solid; yield 2.50 g (25%); m.p. 108 °C. $C_{28}H_{42}O_2Se_2$ (568.56 g mol^{-1}): calcd. C 59.15, H 7.45; found C 58.9, H 7.6. ESI-MS (in positive ion mode, methanol) *m*/*z* = 593.05 (100%, $[H_2L^{Se–Se}+Na]^+$). ^{1}H NMR (300 MHz, $CDCl_3$): δ = 1.24 (s, 9 H), 1.42 (s, 9 H), 1.63 (s, 18 H), 6.28 (s, 2 H, OH), 7.30, 7.31 (m, 4 H) ppm. ^{13}C NMR (75 MHz, $CDCl_3$): δ = 29.73, 31.57, 34.45, 35.42, 117.21, 125.56, 129.81, 135.86, 143.48, 151.74 ppm.

2,2′-Dithiobis(4,6-di-*tert*-butylphenol), $H_2L^{S–S}$: To a solution of 2,4-di-*tert*-butylphenol (15.8 g, 76.7 mmol) in toluene (30 mL) was added, over a period of 2 h and at room temperature, a solution of S_2Cl_2 (3.42 mL, 43.3 mmol) in toluene (20 mL). The reaction mixture was stirred at 80 °C for an additional 90 min. The solvent was evaporated and the viscous, orange-brown crude product was dissolved in hot ethanol. The solution was cooled and the product extracted and then recrystallized from CH_3OH as a light yellow compound; yield 5.8 g (32%); m.p. 140 °C. $C_{28}H_{42}O_2S_2$ (474.76 g mol^{-1}): calcd. C 70.84, H 8.92, S 13.51; found C 70.9, H 8.7, S 12.9. ^{1}H NMR (300 MHz, $CDCl_3$): δ = 1.28 (s, 18 H), 1.41 (s, 18 H), 6.52 (s, 2 H, OH), 7.40–7.47 (m, 4 H) ppm. EI-MS: *m*/*z* (%) = 474(44) [M^+].

$[Fe_2L^{Se}_2(\mu\text{-}OCH_3)_2(CH_3OH)_2]$ (1): The ligand H_2L^{Se} (0.49 g, 1 mmol) was dissolved in dry CH_3OH (40 mL). To this mixture Bu_4NOCH_3 (2.5 mL, 20% methanolic solution) was added and the solution stirred under argon for 5 min. To this, a yellow solution of $FeCl_2$ (0.13 g, 1 mmol) was added and the resulting brown solution was refluxed under argon for 0.5 h. After cooling, the solution was opened to air and stirred for another 15 min. A deep brown microcrystalline compound was isolated by filtration and air-dried. X-ray diffraction quality crystals of **1**·7CH_3OH were grown from a solvent mixture of CH_2Cl_2 and CH_3OH (1:1); yield 0.35 g (49%). **1**·4CH_3OH (1341.16 g mol^{-1}): calcd. C 57.31, H 8.27; found C 57.6, H 8.2. IR: $\tilde{\nu}$ = 3442(br), 2955–2817(s), 1433(s), 1287–1255(s), 1042, 1014, 835, 733, 565. Absorption spectrum (CH_2Cl_2) λ_{max} (nm), ε (M^{-1} cm^{-1}): 484, 3600.

$Bu_4N[FeL^{Se}_2]$ (2): The ligand H_2L^{Se} (0.49 g, 1 mmol) was dissolved in dry CH_3OH (30 mL). To this mixture Bu_4NOH (3 mL, 1 M methanolic solution) was added and the solution stirred under argon for 5 min. To this, a yellow solution of $FeCl_2$ (0.065 g, 0.5 mmol) was added and the resulting red solution was refluxed under nitrogen for 0.5 h. After cooling, the solution was opened to air and stirred for another 15 min. The solution was then filtered to remove any insoluble solid and the filtrate was kept under a slow sweep of nitrogen gas. Deep red crystals were isolated from the solution within 2 d; yield 0.55 g (86%). $C_{72}H_{116}FeNO_4Se_2$ (1273.48 g mol^{-1}): calcd. C 67.91, H 9.18, N 1.10; found C 68.1, H 9.2, N 1.2. IR: $\tilde{\nu}$ = 3447 (br), 2949–2872 (s), 1429 (s), 1302 (s), 1094, 835, 731, 536 cm^{-1}. Absorption spectrum (CH_2Cl_2) λ_{max} (nm), ε (M^{-1} cm^{-1}): 463, 9650. ESI-MS (CH_2Cl_2): *m*/*z* = 242.2 (positive, Bu_4N^+), *m*/*z* = 1030.5 (negative, M^-).

$Bu_4N[FeL^{Se\prime}L^{Se}]$ (3): H_2L^{Se} (0.5 mmol, 0.245 g) and $H_2L^{Se–Se}$ (0.5 mmol, 0.285 g) were dissolved in dry CH_3OH (25 mL) under nitrogen. To this mixture a light yellow solution of Bu_4NOCH_3 (2 mL, 20% methanolic solution) was added, which turned the reaction solution deep yellow. After stirring the solution for 15 min under nitrogen, $FeCl_2$ (0.13 g, 1 mmol) was added and the solution immediately turned pink/red. Within 1 h a deep red crystalline complex was isolated from the solution; yield 0.29 g (55%). $C_{58}H_{96}FeNO_3Se_2$ (1069.13 g mol^{-1}): calcd. C 65.16, H 9.05, N 1.31; found C 65.3, H 8.8, N 1.1. IR: $\tilde{\nu}$ = 3447 (br), 2959–2871 (s), 1425 (s), 1280–1253 (s), 1095, 834, 733, 547 cm^{-1}. Absorption spectrum (CH_2Cl_2) λ_{max} (nm), ε (M^{-1} cm^{-1}): 341(sh), 10940; 504, 9650. ESI-MS (CH_2Cl_2): *m*/*z* = 242.2 (positive, Bu_4N^+), *m*/*z* = 827.5 (negative, M^-).

$Bu_4N[FeL^{S\prime}L^{S}]$ (4): Complex **4** was synthesized by a procedure similar to that described for **3** except that H_2L^S and $H_2L^{S–S}$ were used instead of the selenium analogues; yield 0.41 g (84%). $C_{58}H_{96}FeNO_3S_2$ (975.37 g mol^{-1}): calcd. C 71.42, H 9.92, N 1.44, S 6.57; found C 71.1, H 9.8, N 1.5, S 6.6. IR: $\tilde{\nu}$ = 3447 (br), 2960–2872 (s), 1434 (s), 1288–1254 (s), 1102, 835, 741, 549 cm^{-1}. Absorption spectrum (CH_2Cl_2) λ_{max} (nm), ε (M^{-1} cm^{-1}): 492, 7690. ESI–MS (CH_2Cl_2): *m*/*z* = 242.2 (positive, Bu_4N^+), *m*/*z* = 732.4 (negative, M^-).

Acknowledgments

We are grateful to the Deutsche Forschungsgemeinschaft (DFG) and the Department of Science and Technology (DST), India for the financial support. D. S. acknowledges the Council of Scientific and Industrial Research (CSIR), India for a fellowship. Skilful technical assistance of Mrs. H. Schucht, Mr. A. Göbel and Mr. B. Mienert is thankfully acknowledged. This work was initiated by T. K. P. during his stay in Mülheim.

[1] a) S. Dai, C. Schwendtmayer, P. Schürmann, S. Ramaswamy, H. Eklund, *Science* **2000**, *287*, 655–658; b) N. M. Giles, G. I. Giles, C. Jacob, *Biochem. Biophys. Res. Commun.* **2003**, *300*, 1–4; c) C. Jacob, *Nat. Prod. Rep.* **2006**, *23*, 851–863; d) C. Jacob, I. Knight, P. G. Winyard, *Biol. Chem.* **2006**, *387*,1385–1397; e) S. Raina, D. Missiakas, *Annu. Rev. Microbiol.* **1997**, *51*, 179–202; f) C. Jacob, G. I. Giles, N. M. Giles, H. Sies, *Angew. Chem.* **2003**, *115*, 4890–4907; *Angew. Chem. Int. Ed.* **2003**, *42*, 4742–4758.

[2] L. Banci, I. Bertini, V. Calderone, S. Ciofi-Baffoni, S. Mangani, M. Martinelli, P. Palumaa, S. Wang, *Proc. Natl. Acad. Sci. USA* **2006**, *103*, 8595–8600.

[3] See for example: a) R. Hunter, M. Caira, N. Stellenboom, *J. Org. Chem.* **2006**, *71*, 8268–8271; b) M. Kirihara, Y. Asai, S. Ogawa, T. Noguchi, A. Hatano, Y. Hirai, *Synthesis* **2007**, 3286–3289; c) A. Khazaei, M. A. Zolfigol, A. Rostami, *Synthesis* **2004**, 2959–2961.

[4] a) D. Liotta, U. Sunay, H. Santiesteban, W. Markiewicz, *J. Org. Chem.* **1981**, *46*, 2605–2610; b) H. Suzuki, M. Yoshinaga, K.

Takaoka, Y. Hiroi, *Synthesis* **1985**, 497–499; c) K. B. Sharpless, R. F. Laura, *J. Am. Chem. Soc.* **1973**, *95*, 2697–2699.
[5] For a selective example, see: N. Roy, S. Sproules, T. Weyhermüller, K. Wieghardt, *Inorg. Chem.* **2009**, *48*, 3783–3791.
[6] J. M. Gonzales, D. J. Musaev, K. Morokuma, *Organometallics* **2005**, *24*, 4908–4914.
[7] D. Carrillo, *Coord. Chem. Rev.* **1992**, *119*, 137–169.
[8] a) S. Itoh, M. Nagagawa, S. Fukuzumi, *J. Am. Chem. Soc.* **2001**, *123*, 4087–4088; b) J. S. Figueroa, K. Yurkerwich, J. Melnick, D. Buccella, G. Parkin, *Inorg. Chem.* **2007**, *46*, 9234–9244; c) L. Han, X. Bu, Q. Zhang, P. Feng, *Inorg. Chem.* **2006**, *45*, 5736–5738.
[9] For representative examples, see: a) T. K. Paine, T. Weyhermüller, K. Wieghardt, P. Chaudhuri, *Inorg. Chem.* **2002**, *41*, 6538–6540; b) T. K. Paine, T. Weyhermüller, L. D. Slep, F. Neese, E. Bill, E. Bothe, K. Wieghardt, P. Chaudhuri, *Inorg. Chem.* **2004**, *43*, 7324–7338; c) T. K. Paine, T. Weyhermüller, K. Wieghardt, P. Chaudhuri, *Dalton Trans.* **2004**, 2092–2101; d) P. Chaudhuri, K. Wieghardt, T. Weyhermüller, T. K. Paine, S. Mukherjee, C. Mukherjee, *Biol. Chem.* **2005**, *386*, 1023–1033.
[10] M. Hesse, H. Meier, B. Zeeh, in: *Spektroskopische Methode in der Organischen Chemie*, Georg Thieme Verlag, Stuttgart, Germany, **1995**.
[11] A. B. P. Lever, in: *Inorganic Electronic Spectroscopy*, Elsevier, Amsterdam, **1984**.
[12] a) J. D. Walker, R. Poli, *Inorg. Chem.* **1990**, *29*, 756–761; b) R. Viswanathan, M. Palaniandavar, P. Pravakaran, P. T. Muthiah, *Inorg. Chem.* **1998**, *37*, 3881–3884.
[13] a) B. Chiari, O. Piovesana, T. Tarantelli, P. F. Zanazzi, *Inorg. Chem.* **1982**, *21*, 1396–1402; b) J. E. Davies, B. M. Gatehouse, *J. Chem. Soc.*, *D* **1970**, 1166; c) J. A. Bertrand, J. L. Breece, P. G. Eller, *Inorg. Chem.* **1974**, *13*, 927–934; d) J. A. Bertrand, J. L. Breece, A. R. Kalyanaraman, G. J. Long, W. A. Baker Jr., *J. Am. Chem. Soc.* **1970**, *92*, 5233–5234; e) J. A. Bertrand, J. L. Breece, P. G. Eller, *Inorg. Chem.* **1974**, *13*, 125–131; f) M. Gerloch, F. E. Mabbs, *J. Chem. Soc. A* **1967**, 1598–1608; g) E. Fleischer, S. Hawkinson, *J. Am. Chem. Soc.* **1967**, *89*, 720–721.
[14] J. A. Thich, C. Chih Ou, D. Powers, B. Vasiliou, D. Mastropaolo, J. A. Potenza, H. J. Schugar, *J. Am. Chem. Soc.* **1976**, *98*, 1425–1433.
[15] M. R. Snow, J. A. Ibers, *Inorg. Chem.* **1973**, *12*, 249–254.
[16] A. W. Addison, T. N. Rao, J. Reedijk, J. van Rijn, G. C. Verschoor, *J. Chem. Soc., Dalton Trans.* **1984**, 1349–1356.
[17] a) B. S. Synder, G. S. Patterson, A. J. Abrahamson, R. Holm, *J. Am. Chem. Soc.* **1989**, *111*, 5214–5223; b) P. Chaudhuri, M. Winter, P. Fleischhauer, W. Haase, U. Flörke, H.-J. Haupt, *Inorg. Chim. Acta* **1993**, *212*, 241–249.
[18] E. Bill, *julX Program*, Max-Planck-Institut für Bioanorganische Chemie, Mülheim an der Ruhr, Germany, **2008**.
[19] T. Weyhermüller, R. Wagner, P. Chaudhuri, *Eur. J. Inorg. Chem.* **2011**, 2547–2557, and references cited therein.
[20] a) B. Albela, E. Bill, O. Brosch, T. Weyhermüller, K. Wieghardt, *Eur. J. Inorg. Chem.* **2000**, 139–146; b) W. Hibbs, P. J. van Koningsbruggen, A. M. Arif, W. W. Shum, J. S. Miller, *Inorg. Chem.* **2003**, *42*, 5645–5653; c) T. Mochizuki, T. Nogami, T. Ishida, *Inorg. Chem.* **2009**, *48*, 2254–2259.
[21] a) ShelXTL v.6.14, Bruker AXS Inc., Madison, WI, USA, **2003**; b) G. M. Sheldrick, *SADABS*, *Bruker–Siemens Area Detector Absorption and Other Correction*, version 2006/1, University of Göttingen, Germany, **2006**; c) G. M. Sheldrick, *ShelXL97*, University of Göttingen, Germany, **1997**; d) PLATON program suite: A. L. Spek, *Acta Crystallogr., Sect. D* **2009**, *65*, 148–155.
[22] S. D. Pastor, J. D. Spivack, L. P. Steinhuebel, *J. Heterocycl. Chem.* **1984**, *21*, 1285–1287.
[23] a) T. Thompson, S. D. Pastor, G. Rihs, *Inorg. Chem.* **1999**, *38*, 4163–4167; b) T. K. Paine, E. Rentschler, T. Weyhermüller, P. Chaudhuri, *Eur. J. Inorg. Chem.* **2003**, 3167–3178; c) T. K. Paine, T. Weyhermüller, E. Bothe, K. Wieghardt, P. Chaudhuri, *Dalton Trans.* **2003**, 3136–3144.

Received: July 1, 2011
Published Online: November 3, 2011

